$Z\to l_i^{\pm}l_j^{\mp}$ processes in the BLMSSM *

Xing-Xing Dong(董幸幸)[1)] Shu-Min Zhao(赵树民)[2)] Xi-Jie Zhan(展希杰)
Zhong-Jun Yang(杨忠军) Hai-Bin Zhang(张海斌) Tai-Fu Feng(冯太傅)
Department of Physics and Technology, Hebei University, Baoding 071002, China

Abstract: In a supersymmetric extension of the Standard Model (SM) where baryon and lepton numbers are local gauge symmetries (BLMSSM), we investigate the charged lepton flavor violating (CLFV) processes $Z\to l_i^{\pm}l_j^{\mp}$ after introducing new gauginos and right-handed neutrinos. In this model, the branching ratios of $Z\to l_i^{\pm}l_j^{\mp}$ are around (10^{-8}–10^{-10}), which approach the present experimental upper bounds. We hope that the branching ratios for these CLFV processes can be detected in the near future.

Keywords: supersymmetric, charged lepton flavor violation, branching ratios

PACS: 11.30.Pb, 13.38.Dg, 14.60.-z **DOI:** 10.1088/1674-1137/41/7/073103

1 Introduction

Neutrinos have tiny masses and mix with each other, as has been proved by the neutrino oscillation experiments [1–4]. This shows that lepton flavor symmetry is not conserved in the neutrino sector. A new particle around 125 GeV has been detected by the LHC [5–7], with properties close to those of the Higgs boson, a great success for the Standard Model (SM). However, due to the GIM mechanism, the expected rates for charged lepton flavor violating (CFLV) processes [8–10] are very tiny in the SM with massive neutrinos. For example, $Br(Z\to e\mu)\sim Br(Z\to e\tau)\sim 10^{-54}$ and $Br(Z\to \mu\tau)\sim 10^{-60}$ [11–15] are much smaller than the experimental upper bounds. CLFV is forbidden in the SM. In Table 1, we show the present experimental limits and future sensitivities for some CLFV processes. In Ref. [16], the authors consider that future sensitivities for CLFV processes may reach 10^{-11}. At a future circular e^+e^- collider (such as FCC-ee (TLEP)) [17–19], it is estimated that the sensitivities could be improved up to 10^{-13}. Thus, any signal of CLFV would be a hint of new physics, and the study of CLFV processes is an effective approach to explore new physics beyond the SM.

In a simple SM extension, CLFV processes are restricted strongly by the tiny neutrino masses. As an appealing supersymmetric extension of the SM, the minimal supersymmetric standard model (MSSM) [27–30] with R-parity [29] conservation has drawn physicists' attention for a long time. However, the left-handed light neutrinos remain massless, and it cannot explain the discovery of neutrino oscillations. Therefore, more research is ongoing on the light neutrino masses and mixings with MSSM extensions [31–36]. As a supersymmetric extension of the MSSM with local gauged baryon (B) and lepton (L) numbers, the BLMSSM has been introduced [37–40]. In the BLMSSM, the local gauged B must be broken in order to account for the asymmetry of matter and antimatter in the universe. Right-handed neutrinos are introduced to explain the data from neutrino oscillation experiments, hence lepton number is also expected to be broken [39]. In Refs. [39, 41], baryon number and lepton number are local gauged and spontaneously broken at the TeV scale in the BLMSSM.

Table 1. Present experimental limits and future sensitivities for the CLFV processes $Z\to l_i^{\pm}l_j^{\mp}$.

CLFV process	present limit	future sensitivity (TESLA)
$Z\to e\mu$	$<7.5\times10^{-7}$ [20–22]	$\sim2.0\times10^{-9}$ [26]
$Z\to e\tau$	$<9.8\times10^{-6}$ [20, 23, 24]	$\sim(1.3-6.5)\times10^{-8}$ [26]
$Z\to \mu\tau$	$<1.2\times10^{-5}$ [20, 23, 25]	$\sim(0.44-2.2)\times10^{-8}$ [26]

In this work, we continue to analyze the CLFV processes $Z\to l_i^{\pm}l_j^{\mp}(Z\to e\mu, Z\to e\tau, Z\to \mu\tau)$ within

Received 9 February 2017

∗ Supported by Major Project of NNSFC (11535002, 11605037, 11647120, 11275036), Natural Science Foundation of Hebei Province (A2016201010, A2016201069) and Natural Science Fund of Hebei University (2011JQ05, 2012-242), Hebei Key Lab of Optic-Electronic Information and Materials, the Midwest Universities Comprehensive Strength Promotion Project

1) E-mail: dxx_0304@163.com

2) E-mail: zhaosm@hbu.edu.cn

Content from this work may be used under the terms of the Creative Commons Attribution 3.0 licence. Any further distribution of this work must maintain attribution to the author(s) and the title of the work, journal citation and DOI. Article funded by SCOAP³ and published under licence by Chinese Physical Society and the Institute of High Energy Physics of the Chinese Academy of Sciences and the Institute of Modern Physics of the Chinese Academy of Sciences and IOP Publishing Ltd

the BLMSSM. Compared with the MSSM, the neutrino masses in the BLMSSM are not zero. Three heavy neutrinos and three new scalar neutrinos are introduced in this model. A new particle, the lepton neutralino χ_L^0, is also introduced. These new sources enlarge the CLFV processes via loop contributions. Therefore, the expected experimental results for the CLFV processes may be obtained in the near future.

This work is organized as follows. In Section 2, we summarize the BLMSSM briefly, including its superpotential, the general soft SUSY-breaking terms, needed mass matrices and couplings. Section 3 is devoted to the decay widths of the CLFV processes $\mathrm{Z}\rightarrow \mathrm{l}_i^{\pm}\mathrm{l}_j^{\mp}$. In Section 4, we give the corresponding parameters and numerical analysis. The discussion and conclusion are given in Section 5. An Appendix is devoted to the concrete forms of coupling coefficients in Fig. 1.

2 BLMSSM

The local gauge group of BLMSSM $SU(3)_C\otimes SU(2)_L\otimes U(1)_Y\otimes U(1)_B\otimes U(1)_L$ [38, 42, 43] enlarges the SM. In the BLMSSM, the new quark superfields $\hat{Q}_4\sim(3,2,1/6,B_4,0)$, $\hat{U}_4^c\sim(\overline{3},1,-2/3,-B_4,0)$, $\hat{D}_4^c\sim(\overline{3},1,1/3,-B_4,0)$, $\hat{Q}_5^c\sim(\overline{3},2,-1/6,-(1+B_4),0)$, $\hat{U}_5\sim(3,1,2/3,1+B_4,0)$ and $\hat{D}_5\sim(3,1-1/3,1+B_4,0)$ are introduced to cancel the B anomaly. To break baryon number spontaneously, the model introduces Higgs superfields $\hat{\Phi}_B\sim(1,1,0,1,0)$ and $\hat{\varphi}_B\sim(1,1,0,-1,0)$. The new lepton superfields $\hat{L}_4\sim(1,2,-1/2,0,L_4)$, $\hat{E}_4^c\sim(1,1,1,0,-L_4)$, $\hat{N}_4^c\sim(1,1,0,0,-L_4)$, $\hat{L}_5^c\sim(1,2,1/2,0,-(3+L_4))$, $\hat{E}_5\sim(1,1-1,0,3+L_4)$ and $\hat{N}_5\sim(1,1,0,0,3+L_4)$ are introduced to cancel the L anomaly. The exotic Higgs superfields $\hat{\Phi}_L\sim(1,1,0,0,-2)$ and $\hat{\varphi}_L\sim(1,1,0,0,2)$ can break lepton number spontaneously. Here B_4 and L_4 stand for baryon and lepton numbers for a given field respectively. In our numerical calculation, we use $B_4=3/2$ and $L_4=3/2$. The exotic Higgs superfields $\hat{\Phi}_B$, $\hat{\varphi}_B$ and $\hat{\Phi}_L$, $\hat{\varphi}_L$ acquire nonzero vacuum expectation values (VEVs), then the exotic quarks and exotic leptons obtain masses. The model also includes the superfields $\hat{X}\sim(1,1,0,2/3+B_4,0)$ and $\hat{X}'\sim(1,1,0,-(2/3+B_4),0)$ to make exotic quarks unstable. Furthermore, with $\hat{X}$ and $\hat{X}'$ mixing together, the lightest mass eigenstate can be a dark matter candidate.

The superpotential of the BLMSSM is shown as follows [44]

$$\mathcal{W}_{\rm BLMSSM}=\mathcal{W}_{\rm MSSM}+\mathcal{W}_B+\mathcal{W}_L+\mathcal{W}_X, \tag{1}$$

with $\mathcal{W}_{MSSM}$ representing the superpotential of the MSSM. The concrete forms of $\mathcal{W}_B$, $\mathcal{W}_L$ and $\mathcal{W}_X$ can be obtained in Ref. [44].

In the BLMSSM, the soft breaking terms $\mathcal{L}_{\rm soft}$ are generally given by [38, 39, 44], and only the leptonic terms contribute to our study:

$$\begin{aligned}\mathcal{L}_{\rm soft}=&-(m^2_{\tilde{N}^c})_{IJ}\tilde{N}_I^{c*}\tilde{N}_J^c-m^2_{\Phi_L}\Phi_L^*\Phi_L-m^2_{\varphi_L}\varphi_L^*\varphi_L\\&-\Big(m_L\lambda_L\lambda_L+h.c.\Big)+A_NY_\nu\tilde{L}H_u\tilde{N}^c\\&+A_{N^c}\lambda_{N^c}\tilde{N}^c\tilde{N}^c\varphi_L+B_L\mu_L\Phi_L\varphi_L+h.c.\Big\}.\end{aligned} \tag{2}$$

Here λ_L represents the gaugino of $U(1)_L$. The $SU(2)_L$ doublets H_u and H_d obtain the nonzero VEVs υ_u and υ_d,

$$H_u=\begin{pmatrix}H_u^+\\ \frac{1}{\sqrt{2}}(\upsilon_u+H_u^0+\mathrm{i}P_u^0)\end{pmatrix},$$

$$H_d=\begin{pmatrix}\frac{1}{\sqrt{2}}(\upsilon_d+H_d^0+\mathrm{i}P_d^0)\\ H_d^-\end{pmatrix}. \tag{3}$$

The $SU(2)_L$ singlets Φ_L and φ_L acquire the nonzero VEVs υ_L and $\overline{\upsilon}_L$,

$$\begin{aligned}\Phi_L&=\frac{1}{\sqrt{2}}(\upsilon_L+\Phi_L^0+\mathrm{i}P_L^0),\\ \varphi_L&=\frac{1}{\sqrt{2}}(\overline{\upsilon}_L+\varphi_L^0+\mathrm{i}\overline{P}_L^0).\end{aligned} \tag{4}$$

In the BLMSSM, the mass matrices of lepton neutralinos, neutrinos, sleptons and sneutrinos are introduced as follows.

In the base $(\mathrm{i}\lambda_L,\psi_{\Phi_L},\psi_{\varphi_L})$ [37, 45, 46], the mixing mass matrix of lepton neutralinos is obtained.

$$M_{LN}=\begin{pmatrix}2M_L & 2\upsilon_Lg_L & -2\overline{\upsilon}_Lg_L\\ 2\upsilon_Lg_L & 0 & -\mu_L\\ -2\overline{\upsilon}_Lg_L & -\mu_L & 0\end{pmatrix}. \tag{5}$$

Then the three lepton neutralino masses are deduced by diagonalizing the mass matrix M_{LN} by Z_{N_L}

After symmetry breaking, the mass matrix of neutrinos is deduced in the basis (ν,N^c) [47, 48]

$$\begin{pmatrix}0 & \frac{\upsilon_u}{\sqrt{2}}(\mathrm{Y}_\nu)_{IJ}\\ \frac{\upsilon_u}{\sqrt{2}}(Y_\nu^T)_{IJ} & \frac{\bar{\upsilon}_L}{\sqrt{2}}(\lambda_{N^c})_{IJ}\end{pmatrix}. \tag{6}$$

Then diagonalizing the neutrino mass matrix by the unitary matrix U_ν, we can get six mass eigenstates of neutrinos, which include three light eigenstates and three heavy eigenstates.

In the BLMSSM, the slepton mass squared matrix deduced from Eqs. (1),(2) reads as

$$\begin{pmatrix}(\mathcal{M}_L^2)_{LL} & (\mathcal{M}_L^2)_{LR}\\ (\mathcal{M}_L^2)^\dagger_{LR} & (\mathcal{M}_L^2)_{RR}\end{pmatrix}, \tag{7}$$

where,

$$
\begin{aligned}
(\mathcal{M}_L^2)_{LL} =& \frac{(g_1^2-g_2^2)(v_d^2-v_u^2)}{8}\delta_{IJ}+g_L^2(\bar{v}_L^2-v_L^2)\delta_{IJ} \\
&+m_{lI}^2\delta_{IJ}+(m_{\tilde{L}}^2)_{IJ}, \\
(\mathcal{M}_L^2)_{LR} =& \frac{\mu^* v_u}{\sqrt{2}}(Y_l)_{IJ}-\frac{v_u}{\sqrt{2}}(A_l')_{IJ}+\frac{v_d}{\sqrt{2}}(A_l)_{IJ}, \\
(\mathcal{M}_L^2)_{RR} =& \frac{g_1^2(v_u^2-v_d^2)}{4}\delta_{IJ}-g_L^2(\bar{v}_L^2-v_L^2)\delta_{IJ} \\
&+m_{lI}^2\delta_{IJ}+(m_{\tilde{R}}^2)_{IJ}. \qquad (8)
\end{aligned}
$$

Through the matrix $Z_{\tilde{L}}$, the mass matrix can be diagonalized.

From the contributions of Eqs. (1),(2), we also deduce the mass squared matrix of sneutrino $\mathcal{M}_{\tilde{n}}$ with $\tilde{n}^T=(\tilde{\nu},\tilde{N}^c)$

$$
\begin{pmatrix} \mathcal{M}_{\tilde{n}}^2(\tilde{\nu}_I^*\tilde{\nu}_J) & \mathcal{M}_{\tilde{n}}^2(\tilde{\nu}_I\tilde{N}_J^c) \\ (\mathcal{M}_{\tilde{n}}^2(\tilde{\nu}_I\tilde{N}_J^c))^\dagger & \mathcal{M}_{\tilde{n}}^2(\tilde{N}_I^{c*}\tilde{N}_J^c) \end{pmatrix}, \qquad (9)
$$

where,

$$
\begin{aligned}
\mathcal{M}_{\tilde{n}}^2(\tilde{\nu}_I^*\tilde{\nu}_J) =& \frac{g_1^2+g_2^2}{8}(v_d^2-v_u^2)\delta_{IJ}+g_L^2(\overline{v}_L^2-v_L^2)\delta_{IJ} \\
&+\frac{v_u^2}{2}(Y_\nu^\dagger Y_\nu)_{IJ}+(m_{\tilde{L}}^2)_{IJ}, \\
\mathcal{M}_{\tilde{n}}^2(\tilde{\nu}_I\tilde{N}_J^c) =& \mu^*\frac{v_d}{\sqrt{2}}(Y_\nu)_{IJ}-v_u\overline{v}_L(Y_\nu^\dagger\lambda_{N^c})_{IJ} \\
&+\frac{v_u}{\sqrt{2}}(A_N)_{IJ}(Y_\nu)_{IJ}, \\
\mathcal{M}_{\tilde{n}}^2(\tilde{N}_I^{c*}\tilde{N}_J^c) =& -g_L^2(\overline{v}_L^2-v_L^2)\delta_{IJ}+\frac{v_u^2}{2}(Y_\nu^\dagger Y_\nu)_{IJ} \\
&+2\overline{v}_L^2(\lambda_{N^c}^\dagger\lambda_{N^c})_{IJ}+\mu_L\frac{v_L}{\sqrt{2}}(\lambda_{N^c})_{IJ} \\
&+(m_{\tilde{N}^c}^2)_{IJ}-\frac{\overline{v}_L}{\sqrt{2}}(A_{N^c})_{IJ}(\lambda_{N^c})_{IJ}. \qquad (10)
\end{aligned}
$$

Then the sneutrino masses can be obtained by the formula $Z_{\nu IJ}^\dagger\mathcal{M}_{\tilde{n}}^2 Z_{\nu IJ}=\mathrm{diag}(m_{\tilde{\nu}_1^1}^2,m_{\tilde{\nu}_1^2}^2,m_{\tilde{\nu}_1^3}^2,m_{\tilde{\nu}_2^1}^2,m_{\tilde{\nu}_2^2}^2,m_{\tilde{\nu}_2^3}^2)$.

In the BLMSSM, we deduce the corrections for the couplings which exist in the MSSM due to superfields $\tilde{N}^c$. The corresponding couplings for W-lepton-neutrino, Z-neutrino-neutrino, charged Higgs-lepton-neutrino, Z-sneutrino-sneutrino and chargino-lepton-sneutrino are introduced in Ref. [37].

From the interactions of gauge and matter multiplets $ig\sqrt{2}T_{ij}^a(\lambda^a\psi_jA_i^*-\bar{\lambda}^a\bar{\psi}_iA_j)$, the lepton-slepton-lepton neutralino coupling is deduced here

$$
\begin{aligned}
\mathcal{L}_{l\chi_L^0\tilde{L}} =& \sqrt{2}g_L\bar{\chi}_{L_j}^0\Big(Z_{N_L}^{1j}Z_L^{Ii}P_L \\
&-Z_{N_L}^{1j*}Z_L^{(I+3)i}P_R\Big)l^I\tilde{L}_i^+ + h.c. \qquad (11)
\end{aligned}
$$

3 The CLFV decays $\mathrm{Z}\rightarrow \mathrm{l}_i^{\pm}\mathrm{l}_j^{\mp}$

In the BLMSSM, we study the CLFV processes $\mathrm{Z}\rightarrow \mathrm{l}_i^{\pm}\mathrm{l}_j^{\mp}$. The corresponding Feynman diagrams can be depicted by Fig. 1, and the corresponding effective amplitudes can be written as [15, 49, 50]

$$
\mathcal{M}_\mu=\bar{l}_i\gamma_\mu(F_LP_L+F_RP_R)l_j, \qquad (12)
$$

with

$$
F_{L,R}=F_{L,R}(S)+F_{L,R}(W), \qquad (13)
$$

where $l_{i,j}$ represent the wave functions of the external leptons. The coefficients $F_{L,R}$ can be obtained from the amplitudes of the Feynman diagrams. $F_{L,R}(S)$ correspond to Fig. 1(1)–Fig. 1(7), and stand for the contributions from chargino-sneutrino, neutralino-slepton, neutrino-charged Higgs and lepton neutralino–slepton; $F_{L,R}(W)$ correspond to Fig. 1(8) and Fig. 1(9), and stand for the contributions from W-neutrino due to three light neutrinos and three heavy neutrinos mixing together. We formulate these coefficients as follows:

$$
\begin{aligned}
F_L(S) =& \frac{\mathrm{i}}{2}\sum_{\mathrm{F}=\chi^c,\chi^0,\nu}\sum_{\mathrm{S}=\tilde{\nu},\tilde{\mathrm{L}},\mathrm{H}^\pm(\mathrm{G}^\pm)}\Big[\frac{2m_{F_1}m_{F_2}}{m_{N_p}^2}H_R^{SF_2\bar{l}_i}H_L^{ZF_1\bar{F}_2}H_L^{S^*l_j\bar{F}_1}G_1(x_S,x_{F_1},x_{F_2}) \\
&-H_R^{SF_2\bar{l}_i}H_R^{ZF_1\bar{F}_2}H_L^{S^*l_j\bar{F}_1}G_2(x_S,x_{F_1},x_{F_2})+H_R^{S_2F\bar{l}_i}H^{ZS_1S_2^*}H_L^{S_1^*l_j\bar{F}}G_2(x_F,x_{S_1},x_{S_2})\Big] \\
&+\frac{\mathrm{i}}{2}\sum_{\mathrm{F}=\chi_L^0}\sum_{\mathrm{S}=\tilde{\mathrm{L}}}[H_R^{S_2F\bar{l}_i}H^{ZS_1S_2^*}H_L^{S_1^*l_j\bar{F}}G_2(x_F,x_{S_1},x_{S_2})], \\
F_R(S) =& F_L(S)|_{L\leftrightarrow R}; \\
F_L(W) =& \mathrm{i}\sum_{\mathrm{F}=\nu}\sum_{\mathrm{W}=\mathrm{W}_\mu}[3H_L^{W_2F\bar{l}_i}H^{ZW_1W_2^*}H_L^{W_1^*l_j\bar{F}}G_2(x_F,x_{W_1},x_{W_2}) \\
&-H_L^{WF_2\bar{l}_i}H_L^{ZF_1\bar{F}_2}H_L^{\bar{F}_1l_jW^*}G_2(x_W,x_{F_1},x_{F_2})], \\
F_R(W) =& 0. \qquad (14)
\end{aligned}
$$

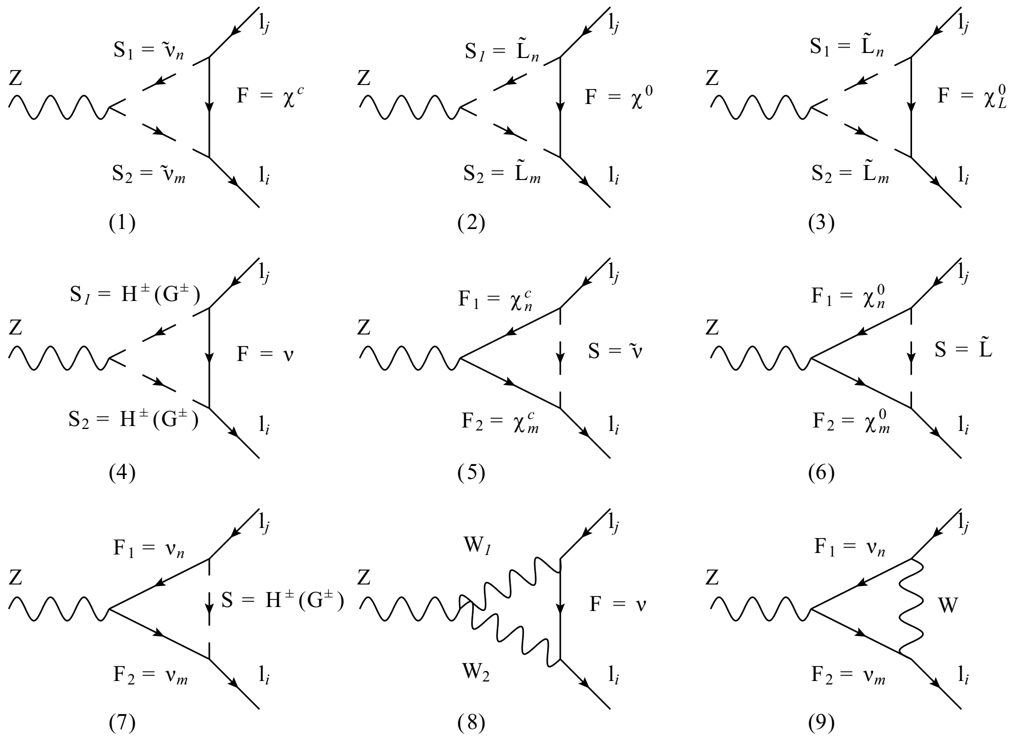

Fig. 1. Feynman diagrams for the $Z\to l_i^{\pm}l_j^{\mp}$ processes in the BLMSSM. F represents Dirac (Majorana) fermions, S represents scalar bosons, and W represents the W boson.

Here, $H_{L,R}^{SF_2\bar{l}_i}$... represent the corresponding coupling coefficients of the left (right)-hand parts in the Lagrangian and the concrete expressions can be found in the Appendix. $x_i=\frac{m^2}{m_{N_p}^2}$, with m representing the mass of the corresponding particle, and m_{N_p} representing the energy scale of the new physics to make the amplitudes dimensionless. The one-loop functions $G_i(x_1,x_2,x_3),i=1,2$ are given by

$$\begin{aligned}G_1(x_1,x_2,x_3) &= \frac{1}{16\pi^2}\left[\frac{x_1\ln x_1}{(x_1-x_2)(x_1-x_3)}+\frac{x_2\ln x_2}{(x_2-x_1)(x_2-x_3)}\right.\\&\left.+\frac{x_3\ln x_3}{(x_3-x_1)(x_3-x_2)}\right],\\G_2(x_1,x_2,x_3) &= \frac{1}{16\pi^2}\left[\frac{x_1^2\ln x_1}{(x_1-x_2)(x_1-x_3)}+\frac{x_2^2\ln x_2}{(x_2-x_1)(x_2-x_3)}\right.\\&\left.+\frac{x_3^2\ln x_3}{(x_3-x_1)(x_3-x_2)}\right].\end{aligned}\quad(15)$$

Then, the branching ratios of $Z\to l_i^{\pm}l_j^{\mp}$ can be summarized as

$$\begin{aligned}Br\left(Z\to l_i^{\pm}l_j^{\mp}\right) &= \frac{1}{12\pi}\frac{m_Z}{\Gamma_Z}\left(|F_L|^2+|F_R|^2\right)\\&= \frac{1}{12\pi}\frac{m_Z}{\Gamma_Z}\left(|F_L(S)+F_L(W)|^2+|F_R(S)|^2\right),\end{aligned}\quad(16)$$

where Γ_Z represents the total decay width of the Z-boson and we use $\Gamma_Z\simeq 2.4952$ GeV [20].

4 Numerical results for the CLFV processes $Z\to l_i^{\pm}l_j^{\mp}$

In this section, we study the numerical results, and consider the experiment constraints from the light neutral Higgs mass $m_{h^0}\simeq 125$ GeV [5–7, 20] and the neutrino experiment data [20]

$$\begin{aligned}&\sin^2\theta_{13}=(2.19\pm0.12)\times10^{-2},\sin^2\theta_{12}=0.304\pm0.014,\\&\sin^2\theta_{23}=0.51\pm0.05,\Delta m_{\odot}^2=(7.53\pm0.18)\times10^{-5}\text{eV}^2,\\&|\Delta m_A^2|=(2.44\pm0.06)\times10^{-3}\text{eV}^2.\end{aligned}\quad(17)$$

In our previous works, the neutron EDM, muon MDM and lepton EDM were studied [45–47], and those constraints are taken into account here. In Refs. [20, 37], $Br(\mu\to e+\gamma)<5.7\times10^{-13}$ and $Br(\mu\to 3e)<1.0\times10^{-12}$ are strict limits for our parameter space. Furthermore, the ratios for $h\to\gamma\gamma$, $h\to ZZ^*$ and $h\to WW^*$ are around 1.16 ± 0.18, $1.29^{+0.26}_{-0.23}$ and $1.08^{+0.18}_{-0.16}$ respectively [20], which are also considered in our parameter space. In this work, the parameters used are [20, 45, 47]:

$$m_e=0.51\times10^{-3}\text{GeV},\ m_Z=91.1876\text{GeV},$$
$$m_\mu=0.105\text{GeV},\ m_\tau=1.777\text{GeV},\ m_W=80.385\text{GeV},$$

$$
\begin{aligned}
&\alpha(m_{\rm Z})=1/128,\ s_{\rm W}^2(m_{\rm Z})=0.23,\\
&(Y_\nu)_{11}=1.3031*10^{-6},\ (Y_\nu)_{12}=9.0884*10^{-8},\\
&(Y_\nu)_{13}=6.9408*10^{-8},\ (Y_\nu)_{22}=1.6002*10^{-6},\\
&(Y_\nu)_{23}=3.4872*10^{-7},\ (Y_\nu)_{33}=1.7208*10^{-6},\\
&L_4=\frac{3}{2},\ \lambda_{N^c}=1. \qquad (18)
\end{aligned}
$$

To simplify the discussion of the numerical result, we assume the following relations

$$
\begin{aligned}
&(A_l)_{ii}=AL,(A_l')_{ii}=A_L',(A_{N^c})_{ii}=(A_N)_{ii}=AN,\\
&(m^2_{\tilde{L}})_{ii}=(m^2_{\tilde{R}})_{ii}=S_m^2,(m^2_{\tilde{N}^c})_{ii}=M_{sn}^2,\\
&(m^2_{\tilde{L}})_{ij}=(m^2_{\tilde{R}})_{ij}=M_{L_f},i\neq j,(i,j=1,2,3) \qquad (19)
\end{aligned}
$$

We choose the parameters $AL=-2$ TeV, $A_L'=300$ GeV, $M_{sn}=1$ TeV, $\tan\beta_L=\bar{v}_L/v_L$ and $V_{L_t}=\sqrt{\bar{v}_L^2+v_L^2}$. m_1 represents the mass of the gaugino in $U(1)$ and m_2 represents the mass of the gaugino in $SU(2)$. Generally, the non-diagonal elements of the parameters are defined as zero unless we note otherwise.

4.1 Z→eμ

The experimental upper bound for the branching ratio of $Z\to e\mu$ is around 7.5×10^{-7}. The parameter m_1 is related to the mass matrix of the neutralino, which means the contributions from neutralino-slepton can be influenced by the parameter m_1. With $g_L=0.3$, $S_m=1$ TeV, $AN=-500$ GeV, $m_2=1$ TeV, $M_{L_f}=1\times10^5$ GeV^2 and $\tan\beta=15$, we plot the results versus m_1 in Fig. 2. As $m_1>0$, the results decrease with increasing m_1. However, the results are in the region ($3.0\times10^{-9}\sim3.5\times10^{-9}$) and the effect of m_1 is small.

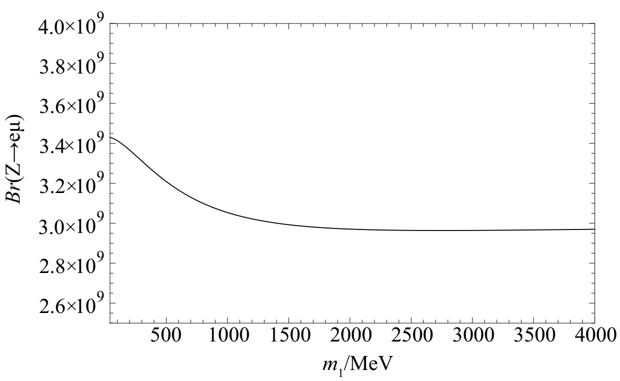

Fig. 2. With $g_L=0.3, S_m=1$ TeV, $AN=-500$ GeV, $m_2=1$ TeV, $M_{L_f}=1\times10^5$ GeV^2 and $\tan\beta=15$, the contributions to $Br(\rm Z\to e\mu)$ versus m_1 are plotted by the solid line.

As a more sensitive parameter, m_2 not only presents in the mass matrix of neutralino, but also in the mass matrix of the chargino. This parameter affects the numerical results through the neutralino-slepton and chargino-sneutrino contributions. In Fig. 3, we show the effects from m_2 with $g_L=0.2$, $S_m=1$ TeV, $AN=-500$ GeV, $\tan\beta=15$ and $M_{L_f}=1\times10^5$ GeV^2. We plot the result with $m_1=500$ GeV, 1000 GeV and 1500 GeV by the solid, dotted and dashed lines respectively. The three lines all become small quickly with increasing m_2. This implies that m_2 is a relatively sensitive parameter to the numerical results.

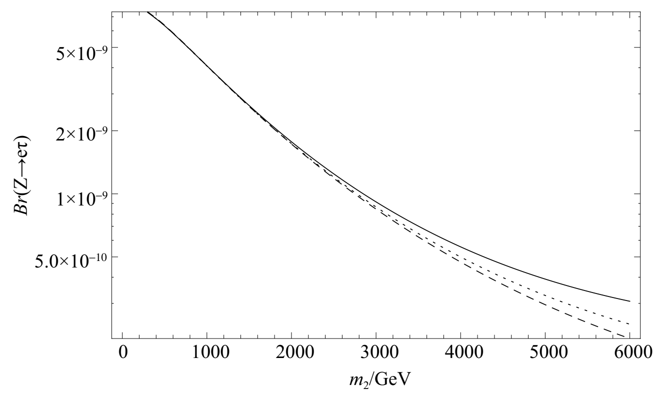

Fig. 3. With $g_L=0.2, S_m=1$ TeV, $AN=-500$ GeV, $\tan\beta=15$, $M_{L_f}=1\times10^5$ GeV^2, $Br(\rm Z\to e\mu)$ versus m_2 is plotted for $m_1=500$ GeV (solid line), 1000 GeV (dotted line), and 1500 GeV (dashed line).

The parameters g_L, $\tan\beta_L$ and V_{L_t} are all present in the mass squared matrices of sleptons, sneutrinos and lepton neutralinos. Therefore, these three parameters affect the results through slepton-neutrino, sneutrinos-chargino and slepton-lepton neutralino contributions. We choose the parameters $m_1=500$ GeV, $m_2=1$ TeV, $S_m=1$ TeV, $AN=500$ GeV and $\tan\beta$=15. As $V_{L_t}=3$ TeV, we plot the allowed results with $\tan\beta_L$ versus g_L in Fig. 4. Obviously, when the value of g_L is large

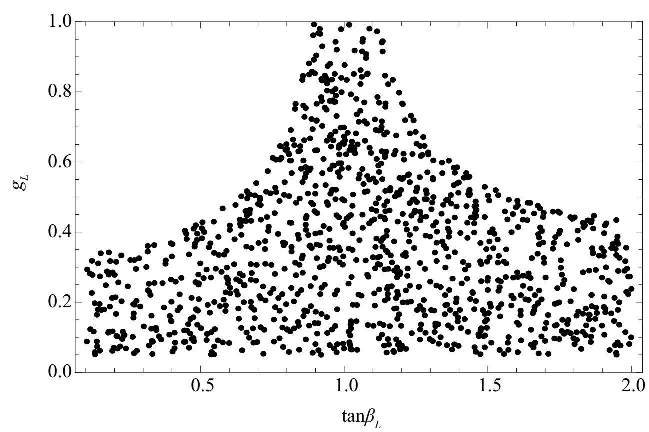

Fig. 4. With $m_1=500$ GeV, $m_2=1$ TeV, $S_m=1$ TeV, AN=500 GeV, $\tan\beta$=15 and V_{L_t}=3 TeV, the allowed parameter space in the plane of $\tan\beta_L$ versus g_L for $Br(\rm Z\to e\mu)$.

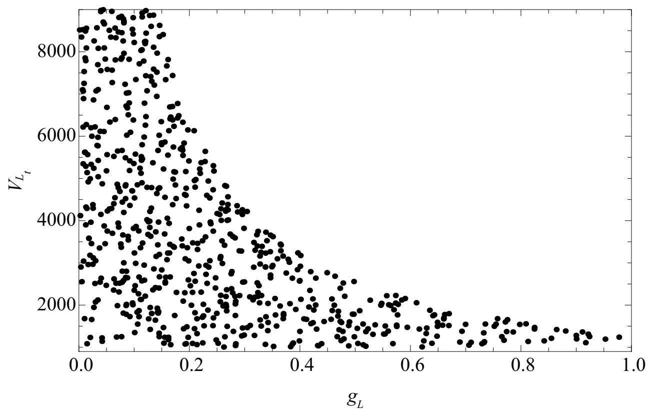

Fig. 5. For $Br(\mathrm{Z}\rightarrow \mathrm{e}\mu)$, the allowed parameter space in the plane of g_L versus V_{L_t} with $m_1=500$ GeV, $m_2=1$ TeV, $S_m=1$ TeV, $AN=500$ GeV, $\tan\beta=15$ and $\tan\beta_L=2$.

enough, the value of $\tan\beta_L$ approaches 1. When $g_L\leqslant 0.3$, the parameter $\tan\beta_L$ can vary in the region of 0–2. This implies that g_L is a sensitive parameter to the numerical results. For $\tan\beta_L=2$, g_L versus V_{L_t} is scanned in Fig. 5. We find that the allowed scope of V_{L_t} shrinks and the value of V_{L_t} decreases with increasing g_L. Therefore, the value of g_L should not be large. Generally, we take $0.05\leqslant g_L\leqslant 0.3$ and $V_{L_t}\sim 3$ TeV in our numerical calculations.

4.2 Z→eτ

In a similar way, the CLFV process Z→eτ is numerically studied and its experimental upper bound is around 9.8×10^{-6}. As discussed in the previous section, g_L can affect the contribution strongly through the masses of sleptons, sneutrinos and lepton neutralinos. S_m is the diagonal element of $m_{\tilde{L}}^2$ and $m_{\tilde{R}}^2$ in the slepton mass matrix, which can affect slepton-neutralino and slepton-lepton neutralino contributions in the CLFV process. Using the parameters $m_1=500$ GeV, $m_2=1$ TeV, $AN=-500$ GeV, $\tan\beta=12$ and $M_{L_f}=1\times 10^5$ GeV^2, we study the branching ratio versus S_m with $g_L=0.1(0.15,0.2)$ in Fig. 6, with the results plotted by the solid line, dotted line and dashed line respectively. These three lines decrease quickly with S_m increasing from 1000 GeV to 2500 GeV, which indicates that S_m is a very sensitive parameter for the numerical results. When $S_m>2500$ GeV, the results decrease slowly and the branching ratios are around $(10^{-9}\sim 10^{-10})$.

We then study the process with the parameters M_{L_f} and m_2. For $S_m=\sqrt{2}$ TeV, $g_L=0.2$, $m_1=500$ GeV, $AN=500$ GeV, and $\tan\beta=12$, we study the results versus M_{L_f} with m_2=1, 1.5, and 2 TeV in Fig. 7, shown by the solid line, dotted line and dashed line respectively. As $M_{L_f}=0$, the branching ratio for $\mathrm{Z}\rightarrow \mathrm{e}\tau$ is almost zero, but the results increase sharply when $|M_{L_f}|>0$. We deduce that non-zero M_{L_f} is a sensitive parameter and has a strong effect on lepton flavor violation.

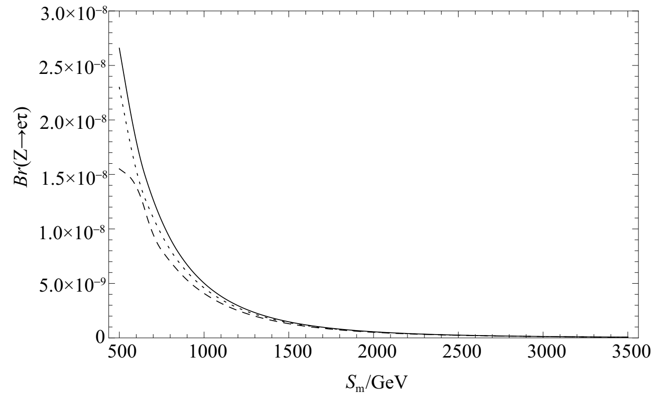

Fig. 6. With $m_1=500$ GeV, $m_2=1$ TeV, $AN=-500$ GeV, $\tan\beta=12$, and $M_{L_f}=1\times 10^5$ GeV^2, the contributions to $Br(\mathrm{Z}\rightarrow \mathrm{e}\tau)$ versus S_m for $g_L=0.1$ (solid line), 0.15 (dotted line), and 0.2 (dashed line).

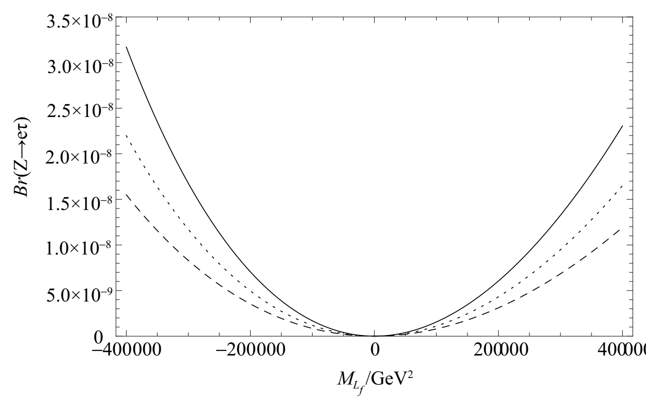

Fig. 7. With $S_m=\sqrt{2}$ TeV, $g_L=0.2$, $m_1=500$ GeV, $AN=500$ GeV, and $\tan\beta=12$, the contributions to $Br(\mathrm{Z}\rightarrow \mathrm{e}\tau)$ versus M_{L_f} for $m_2=1$ TeV (solid line), 1.5 TeV (dotted line), and 2 TeV (dashed line).

4.3 Z→μτ

The experimental upper bound for the CLFV process $\mathrm{Z}\rightarrow\mu\tau$ is 1.2×10^{-5}, which is about one order of magnitude larger than the process $\mathrm{Z}\rightarrow \mathrm{e}\mu$. The parameter AN is present in the sneutrino mass matrix and affects sneutrino-chargino contributions. Supposing $m_1=500$ GeV, $m_2=1$ TeV, $g_L=0.2$, $S_m=1$ TeV, $M_{L_f}=1\times 10^5$ GeV^2 and $\tan\beta=1(2,3)$, we plot the results with the AN in Fig. 8. For $AN\leqslant 4$ TeV, the branching ratios are around 4×10^{-9}. For $AN>4$ TeV, these three lines increase quickly and AN has an obvious influence on the numerical results.

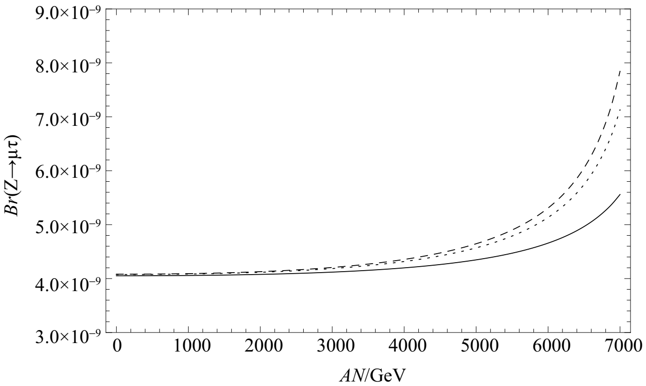

Fig. 8. With $m_1 = 500$ GeV, $m_2 = 1$ TeV, $g_L = 0.2, S_m = 1$ TeV, and $M_{L_f} = 1\times10^5$ GeV^2, the contributions to $Br(\mathrm{Z}\rightarrow\mu\tau)$ versus AN for $\tan\beta = 1$ (solid line), 2 (dotted line), and 3 (dashed line).

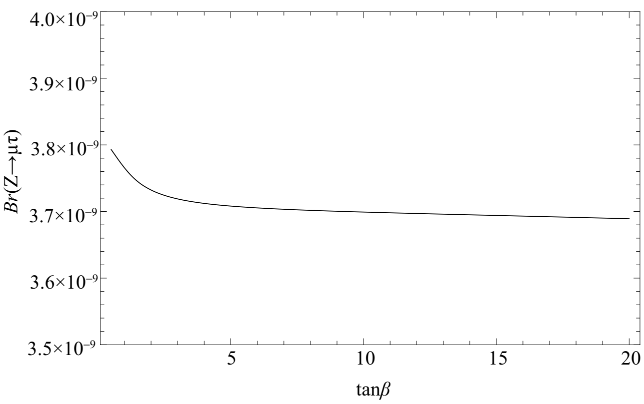

Fig. 9. With $m_1 = 500$ GeV, $m_2 = 1$ TeV, $g_L = 0.3$, $S_m = 1$ TeV, $M_{L_f} = -1\times10^5$ GeV^2, $AN = 500$ GeV, $Br(\mathrm{Z}\rightarrow\mu\tau)$ versus $\tan\beta$ is plotted by the solid line.

Finally, the effects from the parameter $\tan\beta$ are studied. $\tan\beta$ is related to v_u and v_d, and appears in almost all mass matrices of CLFV processes. With $m_1 = 500$ GeV, $m_2 = 1$ TeV, $S_m = 1$ TeV, $g_L = 0.3$, $M_{L_f} = -1\times10^5$ GeV^2 and $AN = 500$ GeV, Fig.9 shows the variation of the branching fraction with the parameter $\tan\beta$. It indicates that the results do not change significantly. In the range of $\tan\beta = (0\sim3)$, we find that the branching ratio decreases slightly; for $\tan\beta > 3$, the result is stable at around 3.7×10^{-9}.

5 Discussion and conclusions

In this paper, we have studied the CLFV processes $\mathrm{Z}\rightarrow \mathrm{l}_i^{\pm}\mathrm{l}_j^{\mp}$ in the BLMSSM. Compared with the MSSM with R-parity conservation, there are new parameters and new contributions to the CLFV processes in the BLMSSM. Firstly, three heavy neutrinos are introduced in this model. However, the new contributions from these particles are tiny, because the couplings of these particles are suppressed by tiny neutrino Yukawa Y_ν. Secondly, three new scalar neutrinos are introduced in this model. Considering the mass squared matrix of the sneutrinos in Eq. (10), we find that the contributions from $\mathcal{M}^2_{\tilde{n}}(\tilde{\nu}_I\tilde{N}^c_J)$ can be neglected due to the tiny Yukawa couplings Y_ν. The effects from $\mathcal{M}^2_{\tilde{n}}(\tilde{\nu}^*_I\tilde{\nu}_J)$ and $\mathcal{M}^2_{\tilde{n}}(\tilde{N}^{c*}_I\tilde{N}^c_J)$ play very important roles. Although the diagonal elements of $(m^2_{\tilde{L}})_{IJ}$ and $(m^2_{\tilde{N}^c})_{IJ}$ suppress the contributions, the non-diagonal element M_{L_f} of $(m^2_{\tilde{L}})_{IJ}$ leads to strong mixing for sneutrinos of different generations. Therefore, the nonzero M_{L_f} enhances lepton flavor violation and leads to large results. Thirdly, lepton neutralinos χ^0_L are the new particles introduced in our work. The numerical results can be influenced by the slepton-lepton neutralino contributions. As the non-diagonal elements, $(\mathcal{M}^2_L)_{LR}$ are not small and can obviously improve the lepton flavor violation effects. Furthermore, the parameters $(m^2_{\tilde{L}})_{IJ}$ and $(m^2_{\tilde{R}})_{IJ}$ respectively exist in $(\mathcal{M}^2_L)_{LL}$ and $(\mathcal{M}^2_L)_{RR}$. It indicates that the non-diagonal element M_{L_f} of $(m^2_{\tilde{L}})_{IJ}$ and $(m^2_{\tilde{R}})_{IJ}$ leads to strong mixing for sleptons. Therefore, $(\mathcal{M}^2_L)_{LR}$ and M_{L_f} influence our results strongly.

In our used parameter space, the numerical results show that the rates for $Br(\mathrm{Z}\rightarrow \mathrm{l}_i^{\pm}\mathrm{l}_j^{\mp})$ can almost reach the present experimental upper bounds. The numerical analyses indicate that parameters $m_1, m_2, g_L, M_{L_f}, S_m, AN$ and $\tan\beta$ are important. The sensitive parameters are g_L, M_{L_f} and S_m and they affect the results strongly. We hope that experimental results for $\mathrm{Z}\rightarrow \mathrm{l}_i^{\pm}\mathrm{l}_j^{\mp}$ can be detected in the near future.

Appendix A

The concrete forms of coupling coefficients corresponding to Fig. 1(1)–Fig. 1(9) are shown as:

Fig.1 (1): $S_1 = \tilde{\nu}_n, S_2 = \tilde{\nu}_m, F = \chi^c$

$$
\begin{aligned}
&H_L^{S_2F\bar{l}_i}(1) = -Y_l^{Im*}Z_-^{2k}Z_{\tilde{\nu}}^{Im},\\
&H_R^{S_2F\bar{l}_i}(1) = -[\frac{e}{s_w}Z_+^{1k*}Z_{\tilde{\nu}}^{Im} + Y_\nu^{Im*}Z_+^{2k*}Z_{\tilde{\nu}}^{(I+3)m}],\\
&H_L^{S_1^*l_j\bar{F}}(1) = -[\frac{e}{s_w}Z_+^{1k}Z_{\tilde{\nu}}^{Jn*} + Y_\nu^{Jn}Z_+^{2k}Z_{\tilde{\nu}}^{(J+3)n*}],\\
&H_R^{S_1^*l_j\bar{F}}(1) = -Y_l^{Jn}Z_-^{2k*}Z_{\tilde{\nu}}^{Jn*},\\
&H^{ZS_1S_2^*}(1) = \frac{e}{2s_wc_w}Z_{\tilde{\nu}}^{Km*}Z_{\tilde{\nu}}^{Kn}.
\end{aligned}
\qquad (\mathrm{A1})
$$

Fig.1 (2): $S_1=\tilde{L}_n, S_2=\tilde{L}_m, F=\chi^0$

$$\begin{aligned}
H_L^{S_2F\bar{l}_i}(2)&=\frac{-\sqrt{2}e}{c_w}Z_L^{(I+3)m*}Z_N^{1k}+Y_l^{I*}Z_L^{Im*}Z_N^{3k},\\
H_R^{S_2F\bar{l}_i}(2)&=\frac{e}{\sqrt{2}s_wc_w}Z_L^{Im*}(Z_N^{1k*}s_w+Z_N^{2k*}c_w)\\
&\quad+Y_l^{I*}Z_L^{(I+3)m*}Z_N^{3k*},\\
H_L^{S_1^*l_j\bar{F}}(2)&=\frac{e}{\sqrt{2}s_wc_w}Z_L^{Jn}(Z_N^{1k}s_w+Z_N^{2k}c_w)\\
&\quad+Y_l^{J}Z_L^{(J+3)n}Z_N^{3k},\\
H_R^{S_1^*l_j\bar{F}}(2)&=\frac{-\sqrt{2}e}{c_w}Z_L^{(J+3)n}Z_N^{1k*}+Y_l^{J}Z_L^{Jn}Z_N^{3k*},\\
H^{ZS_1S_2^*}(2)&=-\frac{e}{2s_wc_w}(Z_L^{Km}Z_L^{Kn*}-2s_w^2\delta^{mn}).
\end{aligned}\tag{A2}$$

Fig.1 (3): $S_1=\tilde{L}_n, S_2=\tilde{L}_m, F=\chi_L^0$

$$\begin{aligned}
H_L^{S_2F\bar{l}_i}(3)&=-\sqrt{2}g_LZ_{N_L}^{1k}Z_L^{(I+3)m*},\\
H_R^{S_2F\bar{l}_i}(3)&=\sqrt{2}g_LZ_{N_L}^{1k*}Z_L^{Im*},\\
H_L^{S_1^*l_j\bar{F}}(3)&=\sqrt{2}g_LZ_{N_L}^{1k}Z_L^{Jn},\\
H_R^{S_1^*l_j\bar{F}}(3)&=-\sqrt{2}g_LZ_{N_L}^{1k*}Z_L^{(J+3)n},\\
H^{ZS_1S_2^*}(3)&=H^{ZS_1S_2^*}(2).
\end{aligned}\tag{A3}$$

Fig.1 (4): $S_1=H^{\pm}(G^{\pm}), S_2=H^{\pm}(G^{\pm}), F=\nu$

$$\begin{aligned}
H_L^{S_2F\bar{l}_i}(4,H)&=-\sin\beta Y_l^{Ik}U_\nu^{Ik},\\
H_R^{S_2F\bar{l}_i}(4,H)&=-\cos\beta Y_\nu^{Ik*}U_\nu^{(I+3)k},\\
H_L^{S_1^*l_j\bar{F}}(4,H)&=-\cos\beta Y_\nu^{Jk}U_\nu^{(J+3)k*},\\
H_R^{S_1^*l_j\bar{F}}(4,H)&=-\sin\beta Y_l^{Jk*}U_\nu^{Jk*},\\
H^{ZS_1S_2^*}(4,H)&=-e\delta^{mn}\frac{c_w^2-s_w^2}{2s_wc_w},\\
H_L^{S_2F\bar{l}_i}(4,G)&=\cos\beta Y_l^{Ik}U_\nu^{Ik},\\
H_R^{S_2F\bar{l}_i}(4,G)&=-\sin\beta Y_\nu^{IK*}U_\nu^{(I+3)k},\\
H_L^{S_1^*l_j\bar{F}}(4,G)&=-\sin\beta Y_\nu^{Jk}U_\nu^{(J+3)k*},\\
H_R^{S_1^*l_j\bar{F}}(4,G)&=\cos\beta Y_l^{Jk*}U_\nu^{Jk*},\\
H^{ZS_1S_2^*}(4,G)&=H^{ZS_1S_2^*}(4,H).
\end{aligned}\tag{A4}$$

Fig.1 (5): $F_1=\chi_n^c, F_2=\chi_m^c, S=\tilde{\nu}$

$$\begin{aligned}
H_L^{SF_2\bar{l}_i}(5)&=-Y_l^{Ik*}Z_-^{2m}Z_{\tilde{\nu}}^{Ik},\\
H_R^{SF_2\bar{l}_i}(5)&=-[\frac{e}{s_w}Z_+^{1m*}Z_{\tilde{\nu}}^{Ik}+Y_\nu^{Ik*}Z_+^{2m*}Z_{\tilde{\nu}}^{(I+3)k}],\\
H_L^{ZF_1\bar{F}_2}(5)&=-\frac{e}{2s_wc_w}[Z_+^{1m*}Z_+^{1n}+\delta^{mn}(c_w^2-s_w^2)],\\
H_R^{ZF_1\bar{F}_2}(5)&=-\frac{e}{2s_wc_w}[Z_-^{1m}Z_-^{1n*}+\delta^{mn}(c_w^2-s_w^2)],\\
H_L^{S^*l_j\bar{F}_1}(5)&=-[\frac{e}{s_w}Z_+^{1n}Z_{\tilde{\nu}}^{Jk*}+Y_\nu^{Jk}Z_+^{2n}Z_{\tilde{\nu}}^{(J+3)k*}],\\
H_R^{S^*l_j\bar{F}_1}(5)&=-Y_l^{Jk}Z_-^{2n*}Z_{\tilde{\nu}}^{Jk*}.
\end{aligned}\tag{A5}$$

Fig.1 (6): $F_1=\chi_n^0, F_2=\chi_m^0, S=\tilde{L}$

$$\begin{aligned}
H_L^{SF_2\bar{l}_i}(6)&=\frac{-\sqrt{2}e}{c_w}Z_L^{(I+3)k*}Z_N^{1m}+Y_l^{I*}Z_L^{Ik*}Z_N^{3m},\\
H_R^{SF_2\bar{l}_i}(6)&=\frac{e}{\sqrt{2}s_wc_w}Z_L^{Ik*}(Z_N^{1m*}s_w+Z_N^{2m*}c_w)\\
&\quad+Y_l^{I*}Z_L^{(I+3)k*}Z_N^{3m*},\\
H_L^{ZF_1\bar{F}_2}(6)&=\frac{e}{2s_wc_w}(Z_N^{4m*}Z_N^{4n}-Z_N^{3m*}Z_N^{3n}),\\
H_R^{ZF_1\bar{F}_2}(6)&=-\frac{e}{2s_wc_w}(Z_N^{4m}Z_N^{4n*}-Z_N^{3m}Z_N^{3n*}),\\
H_L^{S^*l_j\bar{F}_1}(6)&=\frac{e}{\sqrt{2}s_wc_w}Z_L^{Jk}(Z_N^{1n}s_w+Z_N^{2n}c_w)\\
&\quad+Y_l^{J}Z_L^{(J+3)k}Z_N^{3n},\\
H_R^{S^*l_j\bar{F}_1}(6)&=\frac{-\sqrt{2}e}{c_w}Z_L^{(J+3)k}Z_N^{1n*}\\
&\quad+Y_l^{J}Z_L^{Jk}Z_N^{3n*}.
\end{aligned}\tag{A6}$$

Fig.1 (7): $F_1=\nu_n, F_2=\nu_m, S=H^{\pm}(G^{\pm})$

$$\begin{aligned}
H_L^{SF_2\bar{l}_i}(7,H)&=-\sin\beta Y_l^{Im}U_\nu^{Im},\\
H_R^{SF_2\bar{l}_i}(7,H)&=-\cos\beta Y_\nu^{Im*}U_\nu^{(I+3)m},\\
H_L^{ZF_1\bar{F}_2}(7,H)&=-\frac{e}{2s_wc_w}U_\nu^{Km*}U_\nu^{Kn},\\
H_R^{ZF_1\bar{F}_2}(7,H)&=0,\\
H_L^{S^*l_j\bar{F}_1}(7,H)&=-\cos\beta Y_\nu^{Jn}U_\nu^{(J+3)n*},\\
H_R^{S^*l_j\bar{F}_1}(7,H)&=-\sin\beta Y_l^{Jn*}U_\nu^{Jn*},\\
H_L^{SF_2\bar{l}_i}(7,G)&=\cos\beta Y_l^{Im}U_\nu^{Im},\\
H_R^{SF_2\bar{l}_i}(7,G)A_R&=-\sin\beta Y_\nu^{Im*}U_\nu^{(I+3)m},\\
H_L^{ZF_1\bar{F}_2}(7,G)&=H_L^{ZF_1\bar{F}_2}(7,H),\\
H_R^{ZF_1\bar{F}_2}(7,G)&=0,\\
H_L^{S^*l_j\bar{F}_1}(7,G)&=-\sin\beta Y_\nu^{Jn}U_\nu^{(J+3)n*},\\
H_R^{S^*l_j\bar{F}_1}(7,G)&=\cos\beta Y_l^{Jn*}U_\nu^{Jn*}.
\end{aligned}\tag{A7}$$

Fig.1 (8): $W_1=W_1, W_2=W_2, F=\nu$

$$\begin{aligned}
H_L^{W_2F\bar{l}_i}(8)&=-\frac{e}{\sqrt{2}s_w}U_\nu^{Ik},\\
H_L^{W_1^*l_j\bar{F}}(8)&=-\frac{e}{\sqrt{2}s_w}U_\nu^{Jk*},\\
H^{ZW_1W_2^*}(8)&=\frac{ec_w}{s_w},\\
H_R^{W_2F\bar{l}_i}(8)&=H_R^{W_1^*l_j\bar{F}}(8)=0.
\end{aligned}\tag{A8}$$

Fig.1 (9): $F_1=\nu_n, F_2=\nu_m, W=W$

$$\begin{aligned}
H_L^{WF_2\bar{l}_i}(9)&=-\frac{e}{\sqrt{2}s_w}U_\nu^{Im},\\
H_L^{ZF_1\bar{F}_2}(9)&=-\frac{e}{2s_wc_w}U_\nu^{Km*}U_\nu^{Kn},\\
H_L^{\bar{F}_1l_jW^*}(9)&=-\frac{e}{\sqrt{2}s_w}U_\nu^{Jn*},\\
H_R^{WF_2\bar{l}_i}(9)&=H_R^{ZF_1\bar{F}_2}(9)=H_R^{\bar{F}_1l_jW^*}(9)=0.
\end{aligned}\tag{A9}$$

References

1 K. Abe et al (T2K Collab), Phys. Rev. Lett., **107**: 041801 (2011)

2 P. Adamson et al (MINOS Collab), Phys. Rev. Lett., **107**: 181802 (2011)

3 Y. Abe et al (DOUBLE-CHOOZ Collab), Phys. Rev. Lett., **108**: 131801 (2012)

4 F. An et al (DAYA-BAY Collab), Phys. Rev. Lett., **108**: 171803 (2012)

5 ATLAS Collaboration, Phys. Lett. B, **716**: 1 (2012)

6 CMS Collaboration, Phys. Lett. B, **716**: 30 (2012)

7 CMS Collaboration, JHEP, **06**: 081 (2013)

8 A. Abada, D. Das, A. Vicente, and C. Weiland, JHEP, **09**: 015 (2012), arXiv:hep-ph/1206.6497

9 A. Abada, V. De Romeri, and A. M. Teixeira, JHEP, **02**: 083 (2016), arXiv:hep-ph/1510.06657

10 M. Lindner, M. Platscher, F. S. Queiroz, arXiv: hep-ph/1610.06587

11 J.I. Illana, M. Jack and T. Riemann, arXiv:hep-ph/0001273

12 J. I. Illana and T. Riemann, Phys. Rev. D, **63**: 053004 (2001)

13 G. Mann and T. Riemann, Annalen Phys. **40**: 334 (1984)

14 E. O. Iltan and I. Turan, Phys.Rev. D, **65**: 013001 (2002)

15 A. F. Tlalpaa, J. M. Hernandezb, G. T. Velascoa and J. J. Toscanob, Phys.Rev. D, **65**: 073010 (2002)

16 CEPC-SPPC Study Group, "CEPC-SPPC Preliminary Conceptual Design Report", 389 (2015)

17 V. D. Romeri, M. J. Herrero, X. Marcano, and F. Scarcella, arXiv:hep-ph/1607.05257

18 A. Blondel, E. Graverini, N. Serra, and M. Shaposhnikov (FCC-ee study Team), Nucl.Part.Phys.Proc., 273-275 1883-1890 (2016) arXiv:hep-ex/1411.5230

19 A. Abada, V. De Romeri, S. Monteil et al, JHEP, **1504**: 051 (2015), arXiv: hep-ph/1412.6322

20 C. Patrignani et al (Particle Data Group), Chin. Phys. C, **10**: 100001 (2016)

21 G. Aad et al. (ATLAS), Phys. Rev. D, **90**: 072010 (2014)

22 CMS Group, CMS-PAS-EXO-13-005, CERN, (2015)

23 R. Akers et al (OPAL Collaboration), Z. Phys. C, **67**: 555-564 (1995)

24 O. Adriani et al (L3 Collaboration), Phys. Lett. B, **316**: 427 (1993)

25 P. Abreu et al (DELPHI Collaboration), Z. Phys. C, **73**: 243 (1997)

26 G. Wilson, "Neutrino oscillations: are lepton-flavor violating Z decays observable with the CDR detector?" and "Update on experimental aspects of lepton-flavour violation", talks at DESY-ECFA LC Workshops held at Frascati, Nov 1998 and at Oxford, March 1999, transparencies obtainable at http://wwwsis.lnf.infn.it/talkshow/ and at http://hepnts1.rl.ac.uk/ECFA DESY OXFORD/scans/0025 wilson.pdf

27 J. Rosiek, Phys. Rev. D, **41**: 3464 (1990)

28 T.F. Feng and X.Y. Yang, Nucl. Phys. B, **814**: 101 (2009)

29 H.P. Nilles, Phys. Rept., **110**: 1 (1984)

30 H.E. Haber and G.L. Kane, Phys. Rept., **117**: 75 (1985)

31 D. F. Carvalho, J. Ellis, M. E. Gomez, and S. Lola, Phys. Lett. B, **515**: 323–332 (2001)

32 A. Ilakovac and A. Pilaftsis, Nucl. Phys. Proc. Suppl., **218**: 26–31 (2011)

33 J. J. Cao, L. Wu and J. M. Yang, Nucl. Phys. B, **829**: 370–382 (2010)

34 A. Ilakovac , A. Pilaftsis, and L. Popov, Phys. Rev. D, **87**: 5 (2013)

35 H. B. Zhang, T. F. Feng, L.N. Kou, et al, Int. J. Mod. Phys. A, **28**: 1350117 (2013)

36 H. B. Zhang, T. F. Feng, S.M. Zhao, et al, Int. Chin. Phys. C, **41**: 043106 (2017)

37 S.M. Zhao, T.F. Feng, H.B. Zhang, et al, Phys. Rev. D, **92**: 115016 (2015)

38 P. F. Perez and M. B. Wise, Phys. Rev. D, **84**: 055015 (2011)

39 P. F. Perez and M. B. Wise, JHEP, **1108**: 068 (2011)

40 P. F. Perez and M. B. Wise, Phys. Rev. D, **82**: 011901 (2010)

41 T. R. Dulaney, P. F. Perez, M. B. Wise, Phys. Rev. D, **83**: 023520 (2011)

42 P. F. Perez, Phys. Lett. B, **711**: 353 (2012)

43 J.M. Arnold, P. F. Perez, B. Fornal, and S. Spinner, Phys. Rev. D, **85**: 115024 (2012)

44 T. F. Feng, S. M. Zhao, H. B. Zhang et al, Nucl. Phys. B, **871**: 223 (2013)

45 S.M. Zhao, T.F. Feng, H.B. Zhang et al, JHEP, **1507**: 124 (2015)

46 S.M. Zhao, T.F. Feng, B. Yan et al, JHEP, **10**: 020 (2013)

47 S.M. Zhao, T.F. Feng, H.B. Zhang et al, JHEP, **1411**: 119 (2014)

48 X.X. Dong, S.M. Zhao,H.B. Zhang et al, Chin. Phys. C, **40**: 093103 (2016)

49 J. Hisano, T. Moroi, K. Tobe and M. Yamaguchi, Phys. Rev. D, **53**: 2442–2459 (1996)

50 H. B. Zhang, T. F. Feng, S. M. Zhao and F. Sun, Int. J. Mod. Phys. A, **29**: 1450123 (2014)